

Fractal Mobile/Immobile Solute Transport

Rina Schumer

David A. Benson*

Desert Research Institute, 2215 Raggio Pkwy., Reno, Nevada 89512

Mark M. Meerschaert

Department of Mathematics, University of Nevada, Reno, Nevada 89577-0084

Boris Baeumer

Department of Mathematics and Statistics, University of Otago, Dunedin NZ

* Corresponding Author (dbenson@dri.edu)

Abstract

A fractal mobile/immobile model for solute transport assumes power-law waiting times in the immobile zone, leading to a fractional time derivative in the model equations. The equations are equivalent to previous models of mobile/immobile transport with power-law memory functions and are the limiting equations that govern continuous time random walks with heavy tailed random waiting times. The solution is gained by performing an integral transform on the solution of any boundary value problem for transport in the absence of an immobile phase. In this regard, the output from a multidimensional numerical model can be transformed to include the effect of a fractal immobile phase. The solutions capture the anomalous behavior of tracer plumes in heterogeneous aquifers, including power-law breakthrough curves at late time, and power-law decline in the measured mobile mass. The MADE site mobile tritium mass decline is consistent with a fractional time derivative of order $\gamma = 0.33$, while Haggerty et al.'s [2002] stream tracer test is well modeled by a fractional time derivative of order $\gamma = 0.3$.

1. Introduction

As they move through an aquifer or stream, dissolved solutes may sorb to solids or diffuse into regions where the advective flux is negligible. To sufficiently describe the mobile solute concentrations and masses, some functional relationship between the concentrations in the relatively mobile and immobile regions (phases) must be formulated. Typically, this is done with equilibrium (time-independent) or kinetic relationships in a continuum setting. The earliest efforts along these lines gave the linear retardation factor for instantaneous, equilibrium sorption [Bear, 1972; Reynolds *et al.*, 1982] and first-order kinetic mass transfer, commonly called the mobile/immobile (MIM) model [Coats and Smith, 1964; van Genuchten and Wierenga, 1976]. Both have been successfully applied to a large number of tracer tests. The former predicts rapid decline of the late portion of a breakthrough curve (BTC), while the latter predicts exponential decline. However, several recent field tests that have resolved very low concentrations show breakthrough curves with heavier, power-law, tails (e.g., Becker and Shapiro [2000], Haggerty *et al.*, [2000, 2001, 2002]). In this paper, we develop a parsimonious MIM model with fractal retention times to describe this behavior.

Haggerty and Gorelick [1995] adopted a model that combines a number of kinetic rates, reasoning that diffusion into, and out of, different sized domains will take place at different effective rates. The model is nonlocal in time, reflecting the fact that the immobile phase acts as a filter on the “signal” in the mobile phase. Especially interesting is Haggerty *et al.*'s [2000] fractal, or power-law, distribution of rates. If a classical, single rate model is adopted to describe these tests, it takes on the same sort of scaling property in time that has long been noticed in space: as the timescale of a test grows, the coefficients on the time operators must be adjusted to

match the test. Just as an “effective” dispersivity coefficient on a second-order dispersion term is thought to grow with a plume’s length scale [e.g., *Neuman*, 1995], an “effective” rate coefficient must shrink with the time scale of the test [*Haggerty et al.*, 2000]. On the other hand, a model with a fractional dispersion derivative possesses scale invariance [*Benson et al.*, 2000a] and a model with a constant dispersion coefficient may be able to describe the data from all spatial scales. In the present study we consider a fractal (power law) distribution of rate coefficients that is scale invariant in time and leads to a fractional time derivative in the transport equation. *Haggerty et al.* [2000, 2001, 2002] truncated the fractal distribution of rates to preserve the existence of moments; however, the introduction of the cutoffs is not clearly necessary or implied.

In a different (Lagrangian) setting, an extension of the classical random walk model allows a particle to stop for random amounts of time along its trajectory. This general process is called a continuous time random walk (CTRW). A CTRW may or may not converge to a Brownian motion. *Schumer* [2002] and *Dentz and Berkowitz* [2003] take different approaches to show that the Lagrangian random walk model is equivalent to the continuum mobile/immobile equation in the same way that Brownian motion is equivalent to the diffusion equation. The importance of the equivalence of the CTRW to the MIM is that a great deal is known about the limit processes of the CTRW. The CTRW converges toward a limit that corresponds to a MIM continuum model. The convergence is a property that is useful when making long-term predictions.

A key to the comparison of the Lagrangian and Eulerian methods is that governing equations can be generated for the evolution of the concentration profile in both the mobile and immobile phases (and, therefore, the total resident concentration). This allows us to distinguish between the very different breakthrough curves for total versus mobile concentration. Most

research on CTRW does not make this distinction since it is thought that the particle can be “observed” whether it is mobile or not. However, in a hydrologic setting, we may only be able to measure the solute when it is in a mobile phase, since samples are typically drawn preferentially from mobile water (e.g., groundwater wells, grab samples from a stream). The distinction between mobile and total concentration (or the probabilistic location of a particle in either phase) also allows an analysis of the changes in total mobile mass, which depends on the initial condition in both phases. The single-rate MIM equation predicts an exponential approach to an asymptotic state where the mobile mass remains a constant positive fraction of the injected mass [*Goltz and Roberts, 1987; Harvey and Gorelick, 2000*]. Tracer tests at the MacroDispersion Experiment (MADE) site show a continual decrease in mass recovery [*Adams and Gelhar, 1992; Boggs and Adams, 1992; Harvey and Gorelick, 2000*]. The decrease follows a power-law, which points to a fractal distribution of rate coefficients.

In this study, we generalize classical MIM transport theory and determine the conditions under which the MIM transport equations conserve mass, i.e., describe total (mobile + immobile) solute transport. We also examine the mobile transport equation and determine when mass recovery is incomplete. When the memory function of the mobile/immobile equations follows a power-law, a fractional time derivative of order $0 < \gamma \leq 1$ appears in the governing transport equation. These transport equations govern the long time limits of continuous time random walk (CTRW) models, implying a probabilistic interpretation of the MIM advection-dispersion equations (ADEs). We find that the solutions to the mobile/immobile fractional-in-time transport equations are integral transforms of the “conservative” solution to an integer order (in time) counterpart in which no immobile phase is present. This “conservative” solution may come from any sort of time-homogeneous boundary value problem including one from a

multidimensional, numerical solver. Finally, we discuss key features of tracer tests that the fractional-in-time mobile solute transport model can predict.

2.1 Generalization of Classical Mobile/Immobile Transport Theory

Mobile/immobile phase equations equate the divergence of advective and dispersive flux of a mobile phase to the change in concentration in both the mobile and immobile zones ($C_m(x, t)$ and $C_{im}(x, t)$, respectively), due to some partitioning between the phases [Coats and Smith, 1964]:

$$\frac{\partial C_m}{\partial t} + \beta \frac{\partial C_{im}}{\partial t} = L(x)C_m, \quad (1)$$

where, for example, in the classical 1-D case $L(x) = -v \frac{\partial}{\partial x} + \mathcal{D} \frac{\partial^2}{\partial x^2}$, v is average linear velocity,

and \mathcal{D} is a dispersion coefficient. We will not model chemical sorption in this study, so the

mobile/immobile capacity coefficient can be defined by $\beta = \frac{\theta_{im}}{\theta_m}$, where θ_m and θ_{im} are porosity

in the mobile and immobile zones [Coats and Smith, 1964]. Haggerty and Gorelick [1995] point

out that β is more accurately defined as the ratio of mass in the immobile and mobile phases *at*

equilibrium. This distinction becomes more important when we describe a process that does not

reach equilibrium. The relationship between C_m and C_{im} is typically given by one or more

coupled mass transfer equations [van Genuchten and Wierenga, 1976; Haggerty and Gorelick,

1995]. Haggerty and Gorelick [1995] demonstrate that many of the mobile/immobile and multi-

rate mass transfer equations are related to the linear nonequilibrium mass transfer equation:

$$\frac{\partial C_{im}}{\partial t} = \omega(C_m - C_{im}), \quad (2)$$

where ω is a first-order rate coefficient. The solution to (2) is

$$C_{im} = \omega e^{-\omega t} * C_m + C_{im}(x, 0)e^{-\omega t}, \quad (3)$$

where $*$ denotes convolution: $C_m(x, t) * \omega e^{-\omega t} = \int_0^t C_m(x, t - \tau) \omega e^{-\omega \tau} d\tau$. In this context, it is

apparent that the immobile zone is acting as a filter [Debnath, 1995]. It takes an input function

C_m , and spreads it according to a convolution with an exponential filter function $f(t) = \omega e^{-\omega t}$.

Equation (3) also models the decay (release) of an initial immobile phase according to the same exponential form.

By taking the derivative of (3) with respect to time, we find the linear nonequilibrium mass transfer equation (2) in an alternate form:

$$\frac{\partial C_{im}}{\partial t} = \omega e^{-\omega t} * \frac{\partial C_m}{\partial t} + \omega e^{-\omega t} (C_m(x, 0) - C_{im}(x, 0)). \quad (4)$$

While equations (2) and (4) are equivalent, the latter provides additional information about the evolution of immobile concentration. First, we find that the initial conditions in each phase

affect $\frac{\partial C_{im}}{\partial t}$ for all time. We also see that $f(t) = \omega e^{-\omega t}$ is the “memory function” used by

Carrera et al. [1997] and *Haggerty et al.* [2000]. Both studies demonstrate that the memory

function $f(t)$ can take many forms. In general,

$$\frac{\partial C_{im}}{\partial t} = f(t) * \frac{\partial C_m}{\partial t} + f(t) (C_m(x, 0) - C_{im}(x, 0)). \quad (5)$$

Placing the general mass transfer equation (5) in the conservation of mass equation (1), we have the mobile solute transport equation with general initial condition in both phases:

$$\frac{\partial C_m}{\partial t} + \beta \frac{\partial C_m}{\partial t} * f(t) = L(x)C_m - \beta(C_m(x, 0) - C_{im}(x, 0))f(t). \quad (6)$$

The mass in the mobile phase will increase, decrease, or remain constant, depending on the difference in the initial conditions (i.e., the last term of (6)). If the initial concentration is higher in the mobile phase, it will “leak” into the immobile phase and mobile solute mass will decrease. In general, the initial condition in the immobile zone cannot be ignored.

In a typical tracer test, the solute is placed into the mobile zone, and the immobile zone is initially clean. As a result, most analytical and numerical studies use the initial conditions $C_m(x, 0) = C_{m,0}(x) > 0$ and $C_{im}(x, 0) = 0$, as we will for the remainder of this study. With a clean initial immobile phase, the mobile solute transport equation (6) becomes:

$$\frac{\partial C_m}{\partial t} + \beta \frac{\partial C_m}{\partial t} * f(t) = L(x)C_m - \beta C_{m,0}(x)f(t). \quad (7)$$

While mobile concentration is measured in groundwater or soil column effluent samples, measurements of total (mobile+immobile) concentration C_{tot} are obtained from core samples or other techniques that measure solute in all phases (e.g., time domain reflectometry). To complete our development, we derive the equation for the evolution of immobile solute C_{im} and the evolution of C_{tot} . Solving (5) for C_m and $\frac{\partial C_m}{\partial t}$ and substituting them in (1) yields the immobile solute transport equation:

$$\frac{\partial C_{im}}{\partial t} + \beta \frac{\partial C_{im}}{\partial t} * f(t) = L(x)C_{im} + C_{m,0}(x)f(t). \quad (8)$$

Although advection and dispersion do not occur in the immobile zone, immobile solute evolution is affected by flux in the mobile zone, resulting in an immobile flux term. Note that we have

maintained the assumption of a clean initial condition in the immobile zone: a different equation arises when the initial immobile zone concentration is non-zero.

To obtain the equation describing the transport of total solute C_{tot} , multiply the immobile transport equation (8) by β , add the resulting equation to the mobile transport equation (7), and use

$$C_{tot} = \theta_m C_m + \theta_{im} C_{im} \quad (9)$$

or $\frac{1}{\theta_m} C_{tot} = C_m + \beta C_{im}$ [Jury *et al.*, 1991, p. 230; Sardin *et al.*, 1991], so that

$$\frac{\partial C_{tot}}{\partial t} + \beta \frac{\partial C_{tot}}{\partial t} * f(t) = L(x)C_{tot}, \quad C_{tot}(x, 0) = \theta_m C_{m,0}(x). \quad (10)$$

2.2 Rate of Mass Decline in the Mobile Phase

The total mobile mass with time, $M_m(t)$, in any phase can be computed by integrating the concentration over space to obtain the zeroth spatial moment: $M_m(t) = \int \theta_m C_m(x, t) dx$.

Multiplying through in the mobile solute transport equation (7) by θ_m and integrating over space yields:

$$\frac{\partial M_m}{\partial t} + \beta \frac{\partial M_m}{\partial t} * f(t) = -\beta M_{m,0} f(t). \quad (11)$$

Using the Laplace transform $\tilde{f}(s) = \int_0^\infty e^{-st} f(t) dt$ to solve for the mobile mass M_m leads to:

$$\tilde{M}_m(s) = \frac{M_{m,0}}{s(1 + \beta \tilde{f}(s))}, \quad (12)$$

where $M_{m,0}$ denotes the initial mobile mass. It is clear that the mobile transport equation does

not conserve mass unless, trivially, β or $\tilde{f}(s) = 0$. For example, *Goltz and Roberts* [1987] show

if $f(t) = \omega e^{-\omega t}$, then $M_m(t) = \frac{M_{m,0}}{1+\beta} (1 + \beta e^{-\omega(1+\beta)t})$. Solute mass is transferred from the mobile

to immobile phase with time, and the amount of mass recovered from monitoring wells that preferentially sample the mobile phase decreases.

Total solute mass with time is calculated by integrating (10) over space and noting that the resulting equation $\frac{\partial M_{tot}}{\partial t} + \beta \frac{\partial M_{tot}}{\partial t} * f(t) = 0$, $M_{tot}(x, 0) = \theta_m M_{m,0}(x)$ has constant solution

$M_{tot}(t) = M_{m,0}$. Total solute mass is constant with time and equal to the initial mass. Equation (10), with any memory function, preserves the property of mass-conservative transport.

3. A Power-law Memory Function $f(t)$ and the Fractional-in-Time ADE

Power-law late-time breakthrough curves (BTCs) have been observed during tracer tests in fractured granite and dolomite [*Becker and Shapiro*, 2000; *Haggerty et al.*, 2001; *McKenna et al.*, 2001]; in saturated and unsaturated column experiments [*Farrell and Reinhard*, 1994; *Werth et al.*, 1997; *Callahan et al.*, 2000]; and in surface water flows [*Kirchner et al.*, 2000, 2001; *Haggerty et al.*, 2002]. The power-law tails are associated with power-law decline of mobile solute mass [*Farrell and Reinhard*, 1994], and attributed to a power-law decay in the probability density function describing random waiting times in the immobile zone or a power-law memory function $f(t)$ [*Haggerty et al.*, 2000; *Scher et al.*, 2002; *Dentz and Berkowitz*, 2003; *Schumer*,

2002]. If we let $f(t) = \frac{t^{-\gamma}}{\Gamma(1-\gamma)}$, where $\Gamma(\cdot)$ is the Gamma function, then by definition,

$$\frac{\partial C_m(x, t)}{\partial t} * f(t) = \frac{\partial^\gamma C_m(x, t)}{\partial t^\gamma} \quad (13)$$

is a Caputo fractional derivative of order γ [Mainardi, 1997; Samko et al., 1993]. Using (13) in (7), (8), and (10) results in fractional-in-time ADEs describing total solute transport:

$$\frac{\partial C_{tot}}{\partial t} + \beta \frac{\partial^\gamma C_{tot}}{\partial t^\gamma} = L(x)C_{tot}, \quad C_{tot}(x, 0) = \theta_m C_{m,0}(x), \quad (14)$$

mobile solute transport:

$$\frac{\partial C_m}{\partial t} + \beta \frac{\partial^\gamma C_m}{\partial t^\gamma} = L(x)C_m - \beta C_{m,0}(x) \frac{t^{-\gamma}}{\Gamma(1-\gamma)}, \quad C_m(x, 0) = C_{m,0}(x), \quad (15)$$

and immobile solute transport:

$$\frac{\partial C_{im}}{\partial t} + \beta \frac{\partial^\gamma C_{im}}{\partial t^\gamma} = L(x)C_{im} + C_{m,0}(x) \frac{t^{-\gamma}}{\Gamma(1-\gamma)}, \quad C_{im}(x, 0) = 0. \quad (16)$$

Solutions to these fractional-in-time PDEs exist only when $\gamma \leq 1$ [Schumer, 2002].

The use of fractional-in-time ADEs to model mobile/immobile anomalous solute transport is motivated by four factors: 1) the equations govern the limits of well known stochastic processes, 2) fractional-in-time ADEs describe a combination of first order mass transfer models and reduce to known mobile/immobile equations in the integer order case, 3) the equations have tractable solutions that model the significant features of solute plume evolution in time and space, and 4) the equations are parsimonious, with no more parameters than the classical MIM model. These topics are discussed in the following sections.

3.1 Fractional-in-Time ADEs, Fractional-in-Space ADEs, and Continuous Time Random Walks

The link between the diffusion equation and random walks has long been understood [e.g., Hille and Phillips, 1957]. A Gaussian density is the Green's function solution to the ADE, which describes the location of a particle undergoing Brownian motion. When walks are

generalized to allow very large random trajectories that are heavy tailed, the generalized central limit theorem leads to an ADE with a spatially fractional derivative in the dispersive term [e.g., *Benson et al.*, 2000a; *Meerschaert et al.*, 1999; *Schumer et al.*, 2003]. In the vernacular of this study, a random variable X whose distribution function is approximately a power-law for large values ($\text{Prob}[X > x] \sim x^{-\alpha}$) is called “heavy tailed.” The Green’s function solutions to fractional-in-space ADEs are stable probability densities – skewed to bell-shaped density curves with heavy, power-law tails [*Samorodnitsky and Taqqu*, 1994]. Fractional-in-space ADEs have been used to describe faster-than-Fickian growth rate, skewness, and heavy leading edges of conservative plumes in heterogeneous aquifers [*Benson et al.*, 2000b; *Benson et al.*, 2001]. These authors did not consider partitioning to an immobile phase, which may partially explain discrepancies with the field data [*Lu et al.*, 2002].

A more general framework for the study of particle motion is the CTRW or renewal reward process. A CTRW can be defined as the sum of random particle motions that require a random amount of time to complete [*Montroll and Weiss*, 1965; *Scher and Lax*, 1973; see also the numerous references in the comprehensive review by *Metzler and Klafter*, 2000]. CTRWs are useful models of solute transport in aquifers; a particle can move through the aquifer with groundwater or be motionless due to sorption or immobile zones [e.g., *Berkowitz and Scher*, 1995; *Benson*, 1998; *Berkowitz et al.*, 2001]. When random waiting times have finite mean and are independent of particle trajectory length, CTRWs lead to the same mass-conservative PDEs as their corresponding classical random walks [*Kotulski*, 1995; *Whitt*, 2001]. However, CTRWs with power-law, infinite mean immobile periods are governed in the long time limit by fractional-in-time PDEs [*Barkai et al.*, 2000; *Compte*, 1996; *Meerschaert et al.*, 2002a, 2002b]. The equivalence of the mobile/immobile and certain CTRW models was recently established by

Schumer [2002] and *Dentz and Berkowitz* [2003].

3.2 Relation of Fractional-in-Time ADEs with Classical (Integer-Order) ADEs

When the fractional time derivative is of order $\gamma = 1$, representing instantaneous, reversible mass transfer, the fractional-in-time ADE describing total solute transport (14) reduces to:

$$(1 + \beta) \frac{\partial C_{tot}}{\partial t} = L(x)C_{tot}, \quad C_{tot}(x, 0) = \theta_m C_{m,0}(x), \quad (17)$$

resulting in a linear retardation factor $r = 1 + \beta$. The mobile solute time-fractional ADE (15)

reduces to

$$(1 + \beta) \frac{\partial C_m}{\partial t} = L(x)C_m - \beta C_{m,0}(x)\delta(t), \quad (18)$$

since $\lim_{\gamma \rightarrow 1} \frac{t^{-\gamma}}{\Gamma(1-\gamma)} = \delta(t)$ [*Saichev and Zaslavsky*, 1997], where $\delta(\cdot)$ is a Dirac delta function.

The mobile mass after injection, $M_m(t) = M_{m,0} / (1 + \beta)$, is a constant fraction of the injected mass.

Dimensional analysis in (14) shows that β has units $[T^{\gamma-1}]$, which reduces to a dimensionless β when $\gamma = 1$. The first-order-in-time equation (18) predicts constant mobile mass with time; it describes an instantaneous mass transfer process. The single rate MIM model describes an exponential approach to the equilibrium state. In both cases, the capacity coefficient β has the traditional definition of the ratio of immobile mass to mobile mass at equilibrium [*Haggerty and Gorelick*, 1995]. When $\gamma < 1$, the fractional-in-time model predicts continual transfer of plume mass from the mobile to the immobile phase. Mass transfer between phases never reaches equilibrium because solute continues to encounter new zones (however

small) of clean aquifer. We refer to the conceptual model of multirate diffusion into immobile zones described by *Cunningham et al.* [1997], *Haggerty and Gorelick* [1995], and *Haggerty et al.* [2001] which describes diffusion into immobile matrix blocks of various sizes with unique rate coefficients. Under the fractal model, solute encounters more of the immobile zone porosity with time resulting in an apparent scaling of the immobile porosity to mobile porosity ratio and a capacity coefficient whose units scale with time.

3.3 Late-time Approximations

Haggerty et al. [2000] state that a late-time equation applies when concentration change is more heavily dependent on exchange between the mobile and immobile zones than by advective travel time. Although the fractional-in-time mobile/immobile ADEs have explicit solutions at all times (see Section 0), we present the late-time approximation to the mobile solute fractional ADE because its solution has properties that are easy to identify in field data.

As $t \rightarrow \infty$ (or $s \rightarrow 0$), the term $\frac{\partial C}{\partial t} + \beta \frac{\partial^\gamma C}{\partial t^\gamma}$ (with Laplace transform

$s\tilde{C}(x,s) - C_0 + \beta s^\gamma \tilde{C}(x,s) - \beta s^{\gamma-1} C_0$) converges to $\beta \frac{\partial^\gamma C}{\partial t^\gamma}$ when $0 < \gamma \leq 1$ because $s^\gamma \rightarrow 0$

slower than s . Then the late-time equation corresponding with the total solute transport equation

(14) is:

$$\beta \frac{\partial^\gamma C_{tot}}{\partial t^\gamma} = L(x)C_{tot}, \quad C_{tot}(x,0) = C_{m,0}(x) \quad (19)$$

while the late-time mobile solute transport equation is:

$$\beta \frac{\partial^\gamma C_m}{\partial t^\gamma} = L(x)C_m - \beta C_{m,0}(x) \frac{t^{-\gamma}}{\Gamma(1-\gamma)}, \quad C_m(x,0) = C_{m,0}(x). \quad (20)$$

Since $s \rightarrow 0$ corresponds to $t \rightarrow \infty$, the ratio of the two terms βs^γ and s give an indication of the time at which the late-time approximation can be used. The dimensionless number $\beta t^{1-\gamma}$ is a measure of the relative magnitude of the two operators for large time, and we empirically have found that this number should be greater than 3 (i.e., $t > (3/\beta)^{1/(1-\gamma)}$) for the late time approximation to be used.

4. Solutions to Fractional-in-time ADEs

We present the Green's function solutions ($C(x,0) = \delta(x)$) to the fractional-in-time mobile/immobile ADEs (derived in the Appendix), noting that the solutions to equations with any initial condition can be obtained through convolution with the Green's function solution.

The solutions to fractional-in-time ADEs are integral transforms of the solution of a corresponding "conservative" ADE $c_{conserv}(x,t)$, in which no immobile zone is present, e.g., the

classical ADE $\frac{\partial c_{conserv}(x,t)}{\partial t} = L(x)c_{conserv}(x,t)$. For example, if fluorescent dye and a large

number of oranges were placed in a stream, the oranges would be "conservative" since they cannot penetrate the hyporheic zone. If the dye encountered fractal immobile zones beneath the river, the transport solution would be given by a transform of the "oranges" solution. The same

transforms apply whether mobile flux is Fickian $L(x) = -v \frac{\partial}{\partial x} + \mathcal{D} \frac{\partial^2}{\partial x^2}$ and $c_{conserv}(x,t)$ is

Gaussian (Figure 1), super-Fickian $L(x) = -v \frac{\partial}{\partial x} + \mathcal{D} \frac{\partial^\alpha}{\partial x^\alpha}$, with $0 < \alpha < 2$ and α -stable $c_{conserv}(x,t)$

(Figure 2), or takes any other form in d -dimensions. The solution to the mobile solute transport fractional ADE (15) is:

$$C_m(x, t) = \int_0^t g_\gamma \left(\frac{t-u}{(\beta u)^{1/\gamma}} \right) (\beta u)^{-1/\gamma} c_{conserv}(x, u) du. \quad (21)$$

(Appendix) where $g_\gamma(t)$ is the stable subordinator, whose Laplace transform is e^{-s^γ} (see *Feller*, 1971). The stable subordinator is the density of a heavy tailed random variable that explicitly accounts for the random amount of time spent in the immobile phase. It can be computed using the efficient methods of *Nolan* [1998]. The solutions to the immobile solute and late-time mobile solute fractional ADEs are

$$C_{im}(x, t) = \frac{1}{\gamma} \int_0^t g_\gamma \left(\frac{t-u}{(\beta u)^{1/\gamma}} \right) (\beta u)^{(-1-\gamma)/\gamma} (t-u) c_{conserv}(x, u) du, \text{ and} \quad (22)$$

$$C_{m,late}(x, t) = \int_0^\infty g_\gamma \left(\frac{t}{(\beta u)^{1/\gamma}} \right) (\beta u)^{-1/\gamma} c_{conserv}(x, u) du. \quad (23)$$

Use (9) to solve for total solute concentration. Since $c_{conserv}(x, t)$ can be the solution to any time-homogeneous boundary value problem in 1-, 2-, or 3-D, the solutions to numerical simulations such as MT3D or particle tracking codes can be transformed using (21) to incorporate the effects of immobile zones or kinetic sorption on solute transport. Mathcad sheets that contain these solutions are available from the authors.

Note that $g_\gamma(t)$ is a probability density, so that decreasing the scale parameter results in

$$\lim_{\beta \rightarrow 0} g_\gamma \left(\frac{t-u}{(\beta u)^{1/\gamma}} \right) (\beta u)^{-1/\gamma} = \delta(t-u), \text{ and when } \beta = 0 \text{ we recover the untransformed Green's}$$

function solution of $\frac{\partial c_{conserv}(x, t)}{\partial t} = L(x)c_{conserv}(x, t)$ in every case. In other words, the solution to

the mobile fractional ADE (21) with $\beta = 0$ is $C_m(x, t) = c_{conserv}(x, t)$.

5. Model Properties and Application

The integral solutions to fractional-in-time ADEs described in Section 4 were used to generate the plume snapshots and breakthrough curves shown in this section. A Mathcad worksheet that generates the curves can be obtained from the authors.

5.1 Mobile Mass Decline

Use $\tilde{f}(s) = s^{\gamma-1}$ in the general mobile mass decay equation (12) to find that mass decay predicted by the mobile fractional-in-time ADE (15) is

$$\tilde{M}_m(s) = \frac{M_{m,0}}{s + \beta s^\gamma}. \quad (24)$$

with inverse transform (see the Appendix for details):

$$M_m(t) = M_{m,0} \int_0^t \mathcal{G}_\gamma \left(\frac{t-u}{(\beta u)^{1/\gamma}} \right) (\beta u)^{-1/\gamma} du. \quad (25)$$

As t becomes large (or $s \rightarrow 0$) mobile mass decays (for late-time) according to $\tilde{M}_m(s) \sim \frac{M_{m,0}}{\beta s^\gamma}$,

with inverse transform

$$M_m(t) \sim M_{m,0} \frac{t^{\gamma-1}}{\beta \Gamma(\gamma)}. \quad (26)$$

When $\beta = 1$ and the order of the fractional derivative is $\gamma = 0.5$, mass transfer predicted by the mobile solute transport equation is close to the late-time solution after roughly 10 time units. A larger immobile capacity coefficient β requires less time for convergence (Figure 3).

The MADE site tests, described by *Adams and Gelhar* [1992], *Boggs and Adams* [1992], *Boggs et al.*, [1992], and *Rehfeldt et al.* [1992], were performed in the saturated zone of a highly

heterogeneous alluvial aquifer to validate solute transport models. Analytical equations based on CTRW [Berkowitz and Scher, 1998] or that use only fractional space derivatives [Baeumer et al., 2001; Benson et al., 2001] have been shown to fit normalized data (mass adjusted to equal unity at each snapshot) from the bromide or tritium tracer tests but do not reproduce mass transfer with time. Although no multidimensional fractional model [Meerschaert et al, 1999; Schumer et al., 2003] has been applied to the MADE site data, the discrepancy between non-normalized data and 3-D models [Lu et al., 2002] might partially be explained by the fractional mass transfer shown in this study. Harvey and Gorelick [2000] approximate the MADE site mass decay (using

$$M_m(t) = \frac{1}{1.48} \left(1 + 6e^{\frac{-0.0046(1+6)}{1.48}t} \right), \text{ see Figure 4) and transport using a classical first-order MIM}$$

model. Their model reproduces the plume skewness, but not the heavy (power-law) leading edges of the plume or the power-law decay of mobile mass. The rate of measured mobile mass decline from the MADE-1 bromide plume is well modeled by a fractional time derivative of order $\gamma = 0.33$ and fractal immobile capacity of $\beta = 0.08 t^{-0.67}$ (Figure 4). The mass decline is close to the late-time solution after the second monitoring period at 79 days, as the observed mobile mass fraction decays according to $M_m(t) \approx 25t^{-0.67}$.

Mass recovery estimates in two conservative tracer tests performed at the MADE site initially exceed the injected mass [Adams and Gelhar, 1992; Boggs et al., 1993] and then decrease according to a power-law. While Adams and Gelhar [1992] attributed the early overestimate of mass to experimental error, others attribute it to preferential sampling of the high conductivity areas in which solute is concentrated at early time [e.g. Boggs and Adams, 1992]. The “overrecovery” is due to preferential sampling of the mobile zones where the solute is initially placed, while the calculation of mass reported by Adams and Gelhar [1992] is based on

an assumption of uniform distribution. *Harvey and Gorelick* [2000] support this hypothesis and argue that the transport processes that lead to this bias are significant and should be represented in a transport model. *Harvey and Gorelick* [2000] fit parameters that predict an apparent initial recovery (extrapolated to $t = 0$) of 4.7 times the original mass. The fractal fitting (Figure 4) predicts an apparent mass fraction at $t = 0$ of 5.0.

5.2 Breakthrough Curves

Power-law late-time breakthrough curves (BTC) are the most notable feature of solute transport subject to heavy tailed waiting times due to the immobilization of solute. Researchers have shown the power-law BTC that result from both power-law and gamma (itself a heavy tailed but not scale invariant function) distributions of rate coefficients [*Connaughton et al.*, 1993; *Werth et al.*, 1997; *Haggerty et al.*, 2000]. The analytical solution to the total solute fractional ADE (14) demonstrates that the slope of its log-log late-time breakthrough curve is $-\gamma$, where γ is the order of the fractional time derivative (Figure 5). The immobile solute breakthrough curve has the same log-log slope as the total solute breakthrough curve, but the log-log slope of the mobile solute breakthrough curve (Figure 5) is steeper ($-\gamma-1$).

The late-time BTCs for the MADE site were not measured. Instead we use the power-law BTCs that have been observed in tracer tests of overland stream flow [*Haggerty et al.*, 2002] to test our model. Similar behavior in the spectra of chloride time series at watershed outlets was described by *Kirchner et al.* [2000, 2001] and *Scher et al.* [2001]. *Haggerty et al.* [2002] conducted a tracer test in a 2nd-order mountain stream. They show that the hyporheic zone contains a large range of flowpaths, and that the breakthrough of dye tracer 306.4 m downstream from the release point exhibits a power-law tail. *Haggerty et al.*, [2002] successfully model the

breakthrough with a truncated power-law memory function. We hypothesize that the fractional time derivative (which uses a non-truncated power-law kernel) will model the breakthrough with fewer parameters. We assume that the dye moving within the stream channel is well mixed at a distance of 306 m (peak arrival time of 2600 s) and follows the classical Fickian ADE, so the fractional mobile equation is:

$$\frac{\partial C_m}{\partial t} + \beta \frac{\partial^\gamma C_m}{\partial t^\gamma} = -v \frac{\partial C_m}{\partial x} + \mathcal{D} \frac{\partial^2 C_m}{\partial x^2} - \beta C_{m,0} \delta(x) \frac{t^{-\gamma}}{\Gamma(1-\gamma)}, \quad C_{im}(x, 0) = 0. \quad (27)$$

Haggerty et al., [2002] do not report the mean velocity and dispersion parameters for particles that cannot move out of the stream, so these are left as fitting parameters. An interesting validation exercise would be to simultaneously release large neutral-buoyancy particles to eliminate the fitting of v and \mathcal{D} . The order of the fractional derivative is given by the late-time slope of the BTC, which is approximately $\gamma = 0.3$. Plots of the BTC in log-log and real space show excellent fits (Figure 6) with values of $\beta = 0.0023 \text{ sec}^{\gamma-1}$, $v = 0.12 \text{ m/sec}$, and $\mathcal{D} = 0.2 \text{ m}^2/\text{sec}$, given the initial condition $M_{m,0} = 0.48 \text{ gm/m} \times \delta(x)$. We also show the solution to the classical ADE for a tracer that could not move out of the advective channel flow ($\beta = 0$). Since the mobile transport equation requires $\gamma \leq 1$, it is only applicable to data with mobile solute late-time BTC slope between -1 and -2 . If the slope is steeper than $\sim t^{-2}$, a different model is required. The fractional-in-time model predicts 89% mass recovery compared with a measured mass recovery of 77% [*Haggerty*, 2002].

5.3 Spatial Snapshots

When the Gaussian solution to an ADE is transformed to obtain the total solute fractional-in-time ADE, mass is conserved but retarded (Figure 1). The corresponding solution to the

mobile solute fractional-in-time ADE is close to that of the total solute ADE at its leading edge, but progressively diverges upstream, where some solute is immobilized (Figure 1).

5.3.1 Combination with heavy tailed $c_{conserv}(x,t)$

Transport equations with fractional space derivatives have been shown to model super-Fickian dispersion resulting from infinite-variance particle motion lengths [e.g., *Benson*, 1998; 2000; *Gorenflo and Mainardi*, 1998; *Schumer et al.*, 2001, 2003]. A key feature of the super-Fickian model is heavy tailed leading edges. The slope, on a log-log plot, of the leading edge of the immobile, mobile, and total solute plumes are equal to that of the corresponding integer-order in time, no immobile zone diffusion equation $c_{conserv}(x,t)$ (Figure 7). Theoretically, the slope of the leading edges approach $-1-\alpha$, where α is the order of the spatial derivative [*Benson*, 1998].

5.3.2 Skewness

In addition to decreasing the mobile mass for a given snapshot, increasing β more strongly retards the solute in the mobile phase solution (Figure 8). Large values of β result in a positively skewed plume snapshot as the majority of the mass is held behind the average groundwater velocity. However, small values of β result in a negatively skewed snapshot with a leading edge that decays exponentially as only small amounts of mass are held behind the peak (Figure 8). This means that for small values of β , i.e., small fractions of immobile porosity, heavy tailed leading edges can only result from heavy tailed particle motion lengths and fractional space derivatives. They cannot simply be a result of heavy tailed waiting times (see also *Meerschaert et al.*, [2002b]). For example, at the MADE site, where we estimate $\beta = 0.08 \text{ days}^{-0.67}$, heavy tailed waiting times are not sufficient to produce power-law leading edges and we suspect that a

combination of mobile mass decay and heavy (power-law) leading edges can only be described by a fractional-in-time and space mobile solute ADE.

6. Discussion

Integro-differential equations that contain convolution filters are non-local [*Cushman and Ginn*, 1993; *Muralidhar*, 1993]. Concentration change at a single point in an aquifer governed by fractional-in-space ADEs is a function of the concentration at all points in the aquifer [*Schumer et al.*, 2001]. Fractional-in-time ADEs have memory of the time that solute mass arrives at a given location and releases it accordingly. When the waiting time densities of CTRWs have infinite mean, the limiting equations govern fractal time processes [*Hilfer and Anton*, 1995; *Mandelbrot*, 1982] and predict plumes that have power-law or fractal scaling at late time. The fractional-in-time and space ADE that governs total solute transport at late time (19)

with $L(x) = \mathcal{D} \frac{\partial^\alpha C}{\partial x^\alpha}$ has the convenient space-time scaling property [*Meerschaert et al.*, 2002a]:

$$C_{tot}(x, t) = t^{-\gamma/\alpha} C_{tot}(t^{-\gamma/\alpha} x, 1), \quad (28)$$

and the late-time mobile solute transport equation (20), with this space-fractional $L(x)$ was empirically determined to scale as:

$$C_{m,late}(x, t) = t^{\gamma-1} t^{-\gamma/\alpha} C_m(t^{-\gamma/\alpha} x, 1), \quad (29)$$

which is similar to the scaling of the total solute transport equation (28) but accounts for mass transfer. This scaling is evident in the MADE-1 bromide plume. A 1-D plot of distance versus concentration was generated by taking the maximum concentration within 3 meters of the center line of the plume. Snapshot 3 (day 126) scaled in time by (29) using $\gamma = 0.33$ (from the mass decline data in Figure 4) and $\alpha = 0.9$ (see *Benson et al.*, [2001] and *Baeumer et al.*, [2002])

yields a close fit to the data for days 202, 279, 370, and 503 (Figure 9). Knowledge of the scaling properties alone allows prediction of plume evolution from a single spatial snapshot. This scaling property implies that aquifer heterogeneities act as a fractal filter in space and aquifer immobile zones act as a fractal filter in time.

Simulations of the MADE tracer tests have looked at either heavy tailed motion in 1-D [*Benson et al.*, 2001; *Baeumer et al.*, 2001] or partitioning to an immobile phase [*Berkowitz and Scher*, 1995; *Zheng and Jiao*, 1998; *Feehley et al.*, 2000; *Harvey and Gorelick*, 2000]. An uncalibrated 3-D simulation [*Lu et al.*, 2002] was performed with a model that assumes fractional dispersion in the direction of flow and classical dispersion in the remaining coordinates. The authors of that study point to discrepancies between the simulated and measured plumes, and suggest that a model with a spatially varying velocity field could give a better fit. These simplified studies have provided additional insight into transport processes in highly heterogeneous aquifers but have come up short on providing a comprehensive model of transport. Moment analysis [*Meerschaert et al.*, 2001] and numerical simulation [*Grabasnjak*, 2003] supports heavy tailed, super-Fickian motion in multiple directions. The present study supports heavy tailed partitioning (Section 5.1). Both processes can be combined in a field-scale transport equation [*Schumer et al.*, 2003] with semi-analytic solutions via the subordination integral (21). While no analytic solution can reproduce every nuance of an actual plume, we might expect the fractional approach to capture the essential plume features such as multidimensional skewness, variable scaling rates, the decline of mobile mass, and power-law breakthrough tails. These features arise due to the combined effects of very rapid transport and very long retention times.

7. Conclusions

1. Total solute transport equations have constant mass with time, while mobile solute transport equations with power-law waiting times continually lose mass, since progressively more mass moves out of the mobile zone into the initially clean immobile zone.

2. Fractional-in-time equations arise when the particle waiting times follow a power-law.

3. The solutions to total, mobile, and immobile solute fractional-in-time ADEs are integral transforms of the solution to the corresponding unretarded ADE or fractional-in-space ADE. The transforms are easy to compute and can be performed on the output from analytic or numerical solutions to conservative transport equations that do not model an immobile zone.

4. A fractional-in-time mobile solute ADE models the power-law mass loss in the mobile phase (converging to $\frac{t^{\gamma-1}}{\beta\Gamma(\gamma)}$ for late time) and power-law late-time breakthrough curves

observed in field plumes. The tails of mobile solute breakthrough curves decay as $t^{-\gamma-1}$ while the tails of total solute breakthrough curves decay as $t^{-\gamma}$. A fractional-in-time and space equation can also replicate super-Fickian growth and heavy tailed leading plume edges.

5. Non-integer order fractional time derivatives and fractional space derivatives lead to PDEs that are non-local in time and space. At late time, fractional ADEs have fractal scaling properties that allow prediction of plume evolution without estimation of the velocity, dispersion, or capacity coefficient.

Appendix. The Green's Function Solutions to Fractional-in-Time ADEs

To solve the mobile solute fractional-in-time ADE (15) take its Fourier-Laplace transform:

$$\hat{\tilde{C}}_m(k, s) = \frac{1}{s + \beta s^\gamma - \hat{L}(k)}$$

(where the overhat denotes Fourier and tilde denotes Laplace transform), and use $\frac{1}{b} = \int_0^\infty e^{-bu} du$ to

find

$$\hat{\tilde{C}}_m(k, s) = \int_0^\infty e^{-(s+\beta s^\gamma)u} e^{\hat{L}(k)u} du. \quad (30)$$

We follow the method for solving Cauchy problems of *Baeumer and Meerschaert* [2001]. Start with a transport equation where there is no immobile phase, for example, the classical ADE

$\frac{\partial c_{conserv}(x, t)}{\partial t} = L(x)c_{conserv}(x, t)$. The Green's function solution is the probability density

$c_{conserv}(x, t)$ with Fourier transform $\{c_{conserv}(x, t)\} = e^{\hat{L}(k)t}$. Also note the following Laplace

transforms:

$$\mathcal{L}\{t^{-\gamma}/\Gamma(1-\gamma)\} = s^{\gamma-1},$$

$$\mathcal{L}\left\{\frac{\partial^\gamma C}{\partial t^\gamma}\right\} = \mathcal{L}\left\{\frac{\partial C}{\partial t} * \frac{t^{-\gamma}}{\Gamma(1-\gamma)}\right\} = s^\gamma \tilde{C}(s) - C_0(x)s^{\gamma-1},$$

and

$$\mathcal{L}\left\{H(t-u)g_\gamma\left(\frac{t-u}{(\beta u)^{1/\gamma}}\right)(\beta u)^{-1/\gamma}\right\} = e^{-(s+\beta s^\gamma)u},$$

where $H(\cdot)$ is the Heaviside function and $g_\gamma(t)$ is a stable density with scaling parameter

$0 < \gamma < 1$ (known as a *stable subordinator*) so that $\mathcal{L}\{g_\gamma(t)\} = e^{-s^\gamma}$ [Hille and Phillips, 1957; Baeumer et al., 2001]. Then (30) becomes

$$\tilde{C}_m(x, s) = \int_0^\infty \mathcal{L} \left\{ H(t-u) g_\gamma \left(\frac{t-u}{(\beta u)^{1/\gamma}} \right) (\beta u)^{-1/\gamma} \right\} c_{conserv}(x, u) du,$$

and inverse Laplace transform immediately leads to (21).

Acknowledgements. R.S. was supported by the Desert Research Institute's Sulo and Eileen Maki Fellowship and an American Association of University Women Dissertation Fellowship. D.A.B. was supported by NSF grants DES #9980489 and DMS #0139943 and DOE-BES Grant No. DE-FG03-98ER14885. M.M.M. was partially supported by NSF DES Grant No. 9980484 and NSF DMS Grant No. 0139927. We thank three anonymous reviewers and the associate editor for excellent comments.

References

- Adams, E.E., and L.W. Gelhar, Field study of dispersion in a heterogeneous aquifer 2. Spatial moments analysis, *Water Resour. Res.*, 28 (12), 3293-3397, 1992.
- Baeumer, B., and M.M. Meerschaert, Stochastic solutions for fractional Cauchy problems, *Fractional Calculus and Applied Analysis*, 4 (4), 481-500, 2001.
- Baeumer, B., M.M. Meerschaert, D.A. Benson, and S.W. Wheatcraft, Subordinated advection-dispersion equation for contaminant transport, *Water Resour. Res.*, 37 (6), 1543-1550, 2001.
- Barkai, E., M. R., and J. Klafter, From continuous time random walks to the fractional Fokker-Planck equation, *Phys. Rev. E*, 61, 132-138, 2000.
- Barry, D.A., and G. Sposito, Three-dimensional statistical moment analysis of the Stanford/Waterloo Borden tracer test, *Water Resour. Res.*, 26 (8), 1735-1747, 1990.
- Bear, J., *Dynamics of Fluids in Porous Media*, Dover, New York, 1972.
- Becker, M.W., and A.M. Shapiro, Tracer transport in fractured crystalline rock: Evidence of nondiffusive breakthrough tailing, *Water Resour. Res.*, 36 (7), 1677-1686, 2000.
- Benson, D.A., The fractional advection-dispersion equation: development and application, Ph.D. thesis, University of Nevada, Reno, Nevada, 1998.
- Benson, D.A., S.W. Wheatcraft, and M.M. Meerschaert, The fractional-order governing equation of Lévy motion, *Water Resour. Res.* 36(6), 1413-1423, 2000a.
- Benson, D.A., S.W. Wheatcraft, and M.M. Meerschaert, Application of a fractional advection-dispersion equation, *Water Resour. Res.*, 36 (6), 1403-1412, 2000b.
- Benson, D.A., R. Schumer, M.M. Meerschaert, and S.W. Wheatcraft, Fractional dispersion, Lévy motion, and the MADE tracer tests, *Trans. Por. Media*, 42, 211-240, 2001.

- Berkowitz, B., G. Kosakowski, G. Margolin, and H. Scher, Application of continuous time random walk theory to tracer test measurements in fractured and heterogeneous porous media, *Ground Water*, 39 (4), 593-604, 2001.
- Berkowitz, B., and H. Scher, On characterization of anomalous dispersion in porous and fractured media, *Water Resour. Res.*, 31 (6), 1461-1466, 1995.
- Berkowitz, B., and H. Scher, Theory of anomalous chemical transport in random fracture networks, *Phys. Rev. E*, 57 (5), 5858-5869, 1998.
- Boggs, J.M., and E.E. Adams, Field study of dispersion in a heterogeneous aquifer, 4, investigation of adsorption and sampling bias, *Water Resour. Res.*, 28 (12), 3325-3336, 1992.
- Boggs, J.M., L.M. Beard, and W.R. Waldrop, Transport of tritium and four organic compounds during a natural-gradient experiment (MADE-2), Elect. Power Res. Inst., Palo Alto, Calif., 1993.
- Boggs, J.M., S.C. Young, L.M. Beard, L.W. Gelhar, K.R. Rehfeldt, and E.E. Adams, Field study of dispersion in a heterogeneous aquifer, 1, Overview and site description, *Water Resour. Res.*, 28 (12), 3281-3291, 1992.
- Carrera, J., X. Sanchez-Vila, I. Benet, A. Medina, G. Galarza, and J. Guimera, On matrix diffusion: formulations, solution methods and qualitative effects, *Hydrogeol. J.*, 6 (1), 178-190, 1997.
- Coats, K.H., and B.D. Smith, Dead-end pore volume and dispersion in porous media, *J. Soc. Pet. Eng.*, 4, 73-84, 1964.
- Compte, A., Stochastic foundations of fractional dynamics, *Physical Review E*, 53 (4), 4191-

- 4193, 1996.
- Connaughton, D.F., J.R. Stedinger, L.W. Lion, and M.L. Shuler, Description of time-varying desorption kinetics: Release of naphthalene from contaminated soils, *Environ. Sci. Technol.* 27(12), 2397-2403, 1993.
- Cunningham, J.A., C.J. Werth, M. Reinhard, and P.V. Roberts, Effects of grain-scale mass transfer on the transport of volatile organics through sediments, 1, Model development, *Water Resour. Res.*, 33 (12), 2713-2726, 1997.
- Cushman, J.H., and T.R. Ginn, Nonlocal dispersion in media with continuously evolving scales of heterogeneity, *Trans. Por. Media*, 13, 123-138, 1993.
- Debnath, L., *Integral Transforms and Their Applications*, 457 pp., CRC Press, Boca Raton, 1995.
- Dentz, M., and B. Berkowitz, Transport behavior of a passive solute in continuous time random walks and multirate mass transfer, *Water Resour. Res.* 39(5), doi:10.1029/2001WR001163, 01 May 2003.
- Farrell, J., and M. Reinhard, Desorption of halogenated organics from model solids, sediments, and soil under unsaturated conditions, 2. Kinetics, *Environ. Sci. Technol.*, 28 (1), 63-72, 1994.
- Feehley, C.E., C. Zheng, and F.J. Molz, A dual-domain mass transfer approach for modeling solute transport in heterogeneous aquifers: Application to the Macrodispersion Experiment (MADE) site, *Water Resour. Res.* 36(9), 2501-2516, 2000.
- Feller, W., *An Introduction to Probability Theory and Its Applications*, vol.1, 2nd ed., Wiley, New York, 1971.
- Freyberg, D.L., A natural gradient experiment on solute transport in sand aquifer, 2, Spatial

- moments and the advection and dispersion of nonreactive tracers, *Water Resour. Res.*, *22* (13), 2031-2046, 1986.
- Goltz, M.N., and P.V. Roberts, Using the method of moments to analyze three-dimensional diffusion-limited solute transport from temporal and spatial perspectives, *Water Resour. Res.*, *23* (8), 1575-1585, 1987.
- Gorenflo, R., and F. Mainardi, Random walk models for space-fractional diffusion processes, *Fractional Calculus & Applied Analysis*, *1*, 167-191, 1998.
- Grabasnjak, M., Random particle motion and fractional-order dispersion in highly heterogeneous aquifers, M.S. Thesis, University of Nevada, Reno, Reno, NV, USA, 2003.
- Haggerty, R., and S.M. Gorelick, Multiple-rate mass transfer for modeling diffusion and surface reactions in media with pore-scale heterogeneity, *Water Resour. Res.*, *31* (10), 2383-2400, 1995.
- Haggerty, R., S.A. McKenna, and L.C. Meigs, On the late-time behavior of tracer test breakthrough curves, *Water Resour. Res.*, *36* (12), 3467-3479, 2000.
- Haggerty, R., S.W. Fleming, L.C. Meigs, and S.A. McKenna, Tracer tests in a fractured dolomite, 2. Analysis of mass transfer in single-well injection-withdrawal tests, *Water Resour. Res.*, *37* (5), 1129-1142, 2001.
- Haggerty, R., S.M. Wondzell, M.A. Johnson, Power-law residence time distribution in the hyporheic zone of a 2nd-order mountain stream, *Geophys. Res. Lett.* *29*(10), doi: 10.1029/2002GL014743, 2002.
- Haggerty, R., Personal Communication, 2002.
- Harvey, C., and S.M. Gorelick, Rate-limited mass transfer or macrodispersion: Which dominates plume evolution at the Macrodispersion Experiment (MADE) site?, *Water Resour. Res.*,

- 36 (3), 637-650, 2000.
- Hatano, Y., and N. Hatano, Dispersive transport of ions in column experiments: An explanation of long-tailed profiles, *Water Resour. Res.*, 34 (5), 1027-1033, 1998.
- Hilfer, R., and L. Anton, Fractional master equations and fractal time random walks, *Physical Review E*, 51 (2), R848-R851, 1995.
- Hille, E., and R.S. Phillips, *Functional Analysis and Semi-Groups*, Amer. Math. Soc. Coll. Publ., 31, American Mathematical Society, Providence, 1957.
- Jury, W.A., W.R. Gardner, and W.H. Gardner, *Soil Physics*, 328 pp., John Wiley & Sons, Inc., New York, 1991.
- Kirchner, J. W., X. Feng, and C. Neal, Fractal Stream Chemistry and its implications for contaminant transport in catchments, *Nature* 403, 524-527, 2000.
- Kirchner, J.W., X. Feng, C.E. Renshaw, and C. Neal, Spectral analysis in catchment hydrology and geochemistry, *Eos Trans. AGU*, 82 (47), Abstract H21E-10, 2001.
- Kotulski, M., Asymptotic distributions of the continuous time random walks: A probabilistic approach, *J. Stat. Phys.*, 81, 777-792, 1995.
- Lu, S, F.J. Molz, and G.J. Fix, Possible problems of scale dependency in applications of the three-dimensional fractional advection-dispersion equation to natural porous media, *Water Resour. Res.* 38(9), doi:10.1029/2001WR000624, 2002.
- Mainardi, F., Fractional calculus: some basic problems in continuum and statistical mechanics, in *Fractals and Fractional Calculus in Continuum Mechanics*, edited by A. Carpinteri, and F. Mainardi, pp. 292-348, Springer, New York, 1997.
- Mandelbrot, B., *The Fractal Geometry of Nature*, 460 pp., Freeman, San Francisco, 1982.
- McKenna, S.A., L.C. Meigs, and R. Haggerty, Tracer tests in a fractured dolomite 3. Double-

- porosity, multiple-rate mass transfer processes in convergent flow tracer tests, *Water Resour. Res.*, 37 (5), 1143-1154, 2001.
- Meerschaert, M.M., D.A. Benson, and B. Baeumer, Multidimensional advection and fractional dispersion, *Phys. Rev. E*, 59(5), 5026-5028, 1999.
- Meerschaert, M. M., D.A. Benson, and B. Baeumer, Operator Lévy motion and multiscaling anomalous diffusion. *Phys. Rev. E* 63, 021112-021117, 2001.
- Meerschaert, M.M., D.A. Benson, H.-P. Scheffler, and B. Baeumer, Stochastic solution of space-time fractional diffusion equations, *Phys. Rev. E* 65, 041113-041116, 2002a.
- Meerschaert, M. M., D.A. Benson, P. Becker-Kern, and H.-P. Scheffler, Governing equations and solutions of anomalous random walk limits, *Phys. Rev. E* 66(6), #060102(R), 2002b.
- Metzler, R., and J. Klafter, The random walk's guide to anomalous diffusion: a fractional dynamics approach, *Physics Reports*, 339, 1-77, 2000.
- Montroll, E.W., and G.H. Weiss, Random walks on lattices. II, *J. Math Phys.*, 6 (2), 167-181, 1965.
- Muralidhar, R., Diffusion in pore fractals: a review of linear response models, *TIPM*, 13, 79-95, 1993.
- Neuman, S. P., On advective transport in fractal permeability and velocity fields, *Water Resour. Res.* 31(6), 1455-1460, 1995.
- Nolan, J.P., Multivariate stable distributions: approximation, estimation, simulation and identification, in *A Practical Guide to Heavy Tails: Statistical Techniques and Applications*, edited by R.J. Adler, R. Feldman, and M. Taqqu, Birkhauser, Boston, 1998.
- Rehfeldt, K.R., J.M. Boggs, and L.W. Gelhar, Field study of dispersion in a heterogeneous

- aquifer. 3: Geostatistical analysis of hydraulic conductivity, *Water. Resour. Res.*, 28 (12), 3309-3324, 1992.
- Reynolds, W.D., R.W. Gillham, and J.A. Cherry, Evaluation of distribution coefficients in the prediction of strontium and cesium migration in uniform sand, *Can. Geotech J.* 19, 92-103, 1982.
- Saichev, A.I., and G.M. Zaslavsky, Fractional kinetic equations: solutions and applications, *Chaos*, 7 (4), 753-764, 1997.
- Samko, S.G., A.A. Kilbas, and O.I. Marichev, *Fractional Integrals and Derivatives: Theory and Applications*, 976 pp., Gordon and Breach, London, 1993.
- Samorodnitsky, G., and M.S. Taqqu, *Stable Non-Gaussian Random Processes: Stochastic Models with Infinite Variance*, 632 pp., Chapman Hall, London, 1994.
- Sardin, M., D. Schweich, F.J. Leij, and M.T. vanGenuchten, Modeling the nonequilibrium transport of linearly interacting solutes in porous media: a review, *Water Resour. Res.*, 27 (9), 2287-2307, 1991.
- Scher, H., and M. Lax, Stochastic transport in a disordered solid. I. Theory, *Physical Review B*, 7 (10), 4491-4502, 1973.
- Scher, H, G. Margolin, R. Metzler, J. Klafter, and B. Berkowitz, The dynamical foundation of fractal stream chemistry: The origin of extremely long retention times, *Geophys Res. Lett.* 29(5), doi:10.1029/2001GL014123, 2002.
- Schumer, R., Fractional derivatives, continuous time random walks, and anomalous solute transport, Ph.D. thesis, University of Nevada, Reno, Reno, NV, 2002.
- Schumer, R., D.A. Benson, M.M. Meerschaert, and S.W. Wheatcraft, Eulerian derivation for the fractional advection-dispersion equation, *Journal of Contaminant Hydrology*, 48, 69-88,

2001.

- Schumer, R., D. A. Benson, M. M. Meerschaert, and B. Baeumer, Multiscaling fractional advection-dispersion equations and their solutions, *Water Resour. Res.* 39(1), 1022, doi:10.1029/2001WR001229, 2003.
- vanGenuchten, M.T., and P.J. Wierenga, Mass transfer studies in sorbing porous media, 1, Analytical solutions, *Soil Sci. Soc. Am. J.*, 40, 473-480, 1976.
- Werth, C.J., J.A. Cunningham, P.V. Roberts, and M. Reinhard, Effects of grain-scale mass transfer on the transport of volatile organics through sediments, 2. Column results, *Water Resour. Res.*, 33 (7), 2727-2740, 1997.
- Whitt, W., *Stochastic-Process Limits*, 650 pp., Springer-Verlag, New York, 2001.
- Zheng, C., and J. J. Jiao, Numerical simulation of tracer tests in heterogeneous aquifer, *J. Environ. Eng.* 124(6), 510-516, 1998.

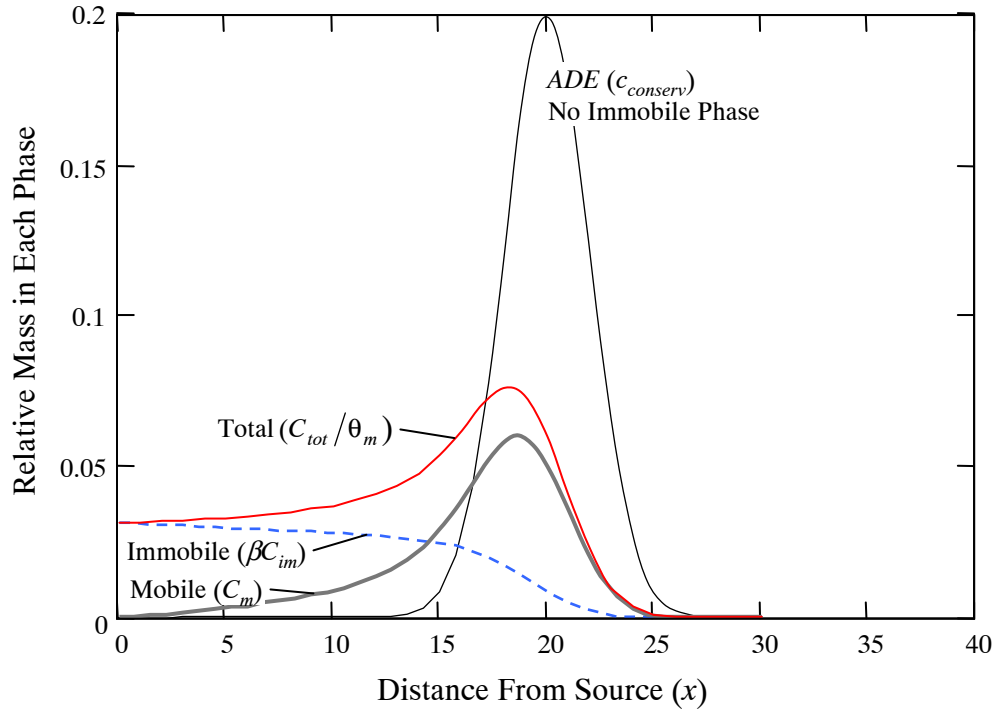


Figure 1. Spatial snapshots, at $t = 20$, of the solution to the unretarded (no immobile phase) classical ADE, along with the total mass, immobile mass, and mobile mass of the retarded (transformed) solutions. ADE parameters are $\nu = 1$ and $\mathcal{D} = 0.1$. The fractional time derivative is order $\gamma = 0.3$ and $\beta = 0.1$ in the retarded transport equations.

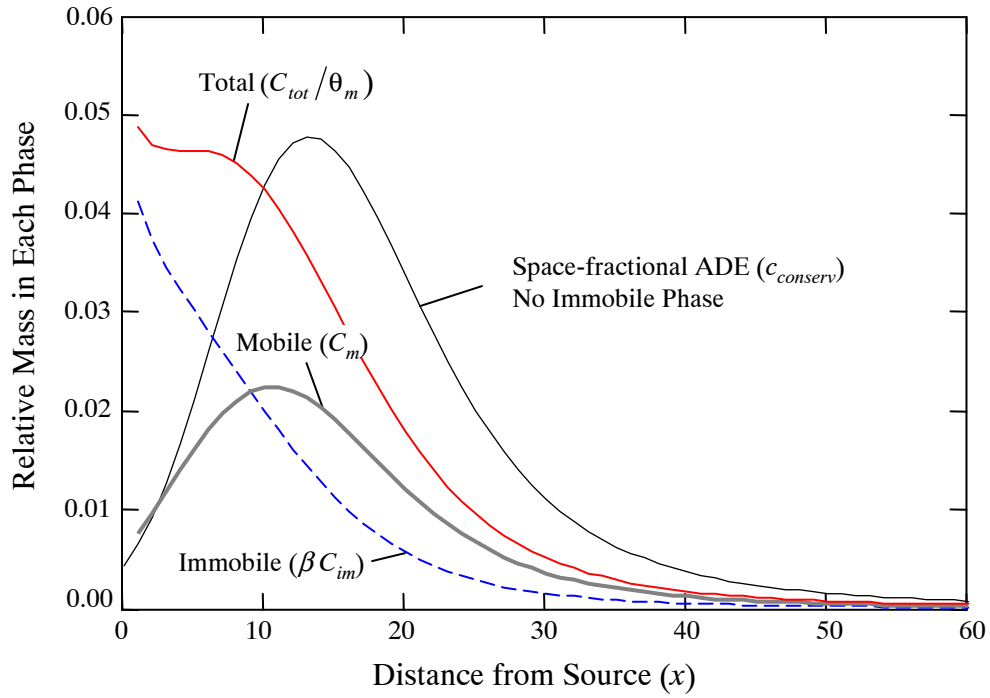


Figure 2. Spatial snapshots, at $t = 20$, of the unretarded (no immobile phase), skewed, 1.5-stable solution to a spatially fractional ADE with $\nu = 1$ and $\mathcal{D} = 0.1$, $\alpha = 1.5$, along with the total mass, immobile mass, and mobile mass of the retarded (transformed) solutions. In the retarded transport equations, the capacity coefficient is $\beta = 0.1$ and the order of the fractional time derivative is $\gamma = 0.3$.

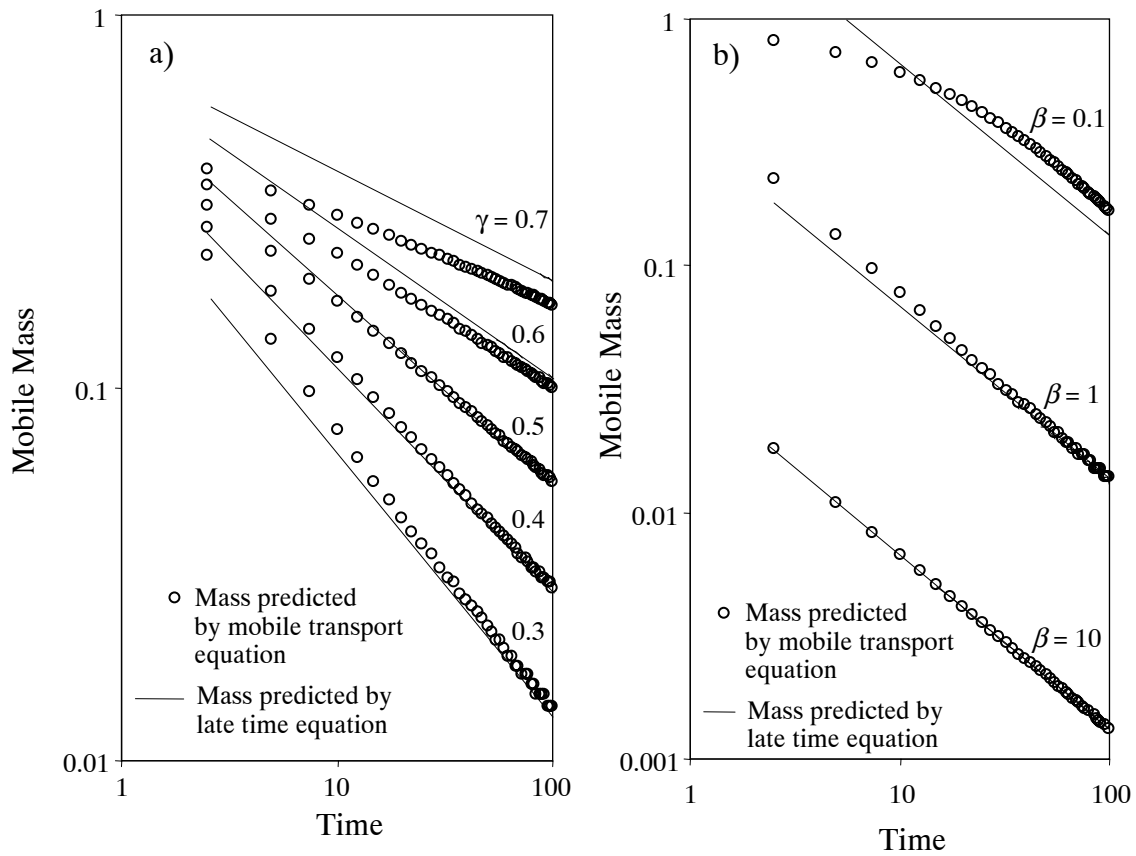


Figure 3. The mobile solute fractional ADE predicts that mass decline converges to $M_m(t) = t^{\gamma-1}/(\beta\Gamma(\gamma))$ with time: a) convergence for various γ when $\beta = 1$, and b) effect of varying β when $\gamma = 0.3$.

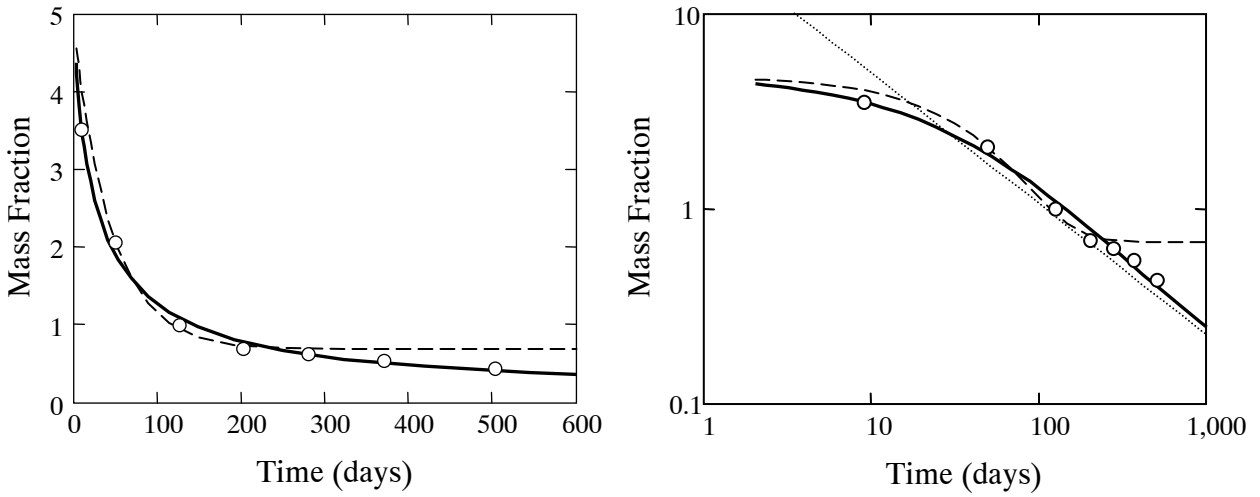


Figure 4. Linear and log-log plots of the observed fraction of injected mass from the MADE-1 bromide plume (circles) compared with a single-rate MIM (dashed line) and the fractal MIM (solid line) models. The fractional time derivative is order $\gamma = 0.33$ and fractal capacity coefficient $\beta = 0.08 d^{-0.67}$. The initial mobile fraction, due primarily to sampling bias, is 5.0 and 4.7 for the fractal and single rate (exponential) models [Harvey and Gorelick, 2000]. Also shown on the log-log plot is the late time approximation (dotted line) given by equation (26).

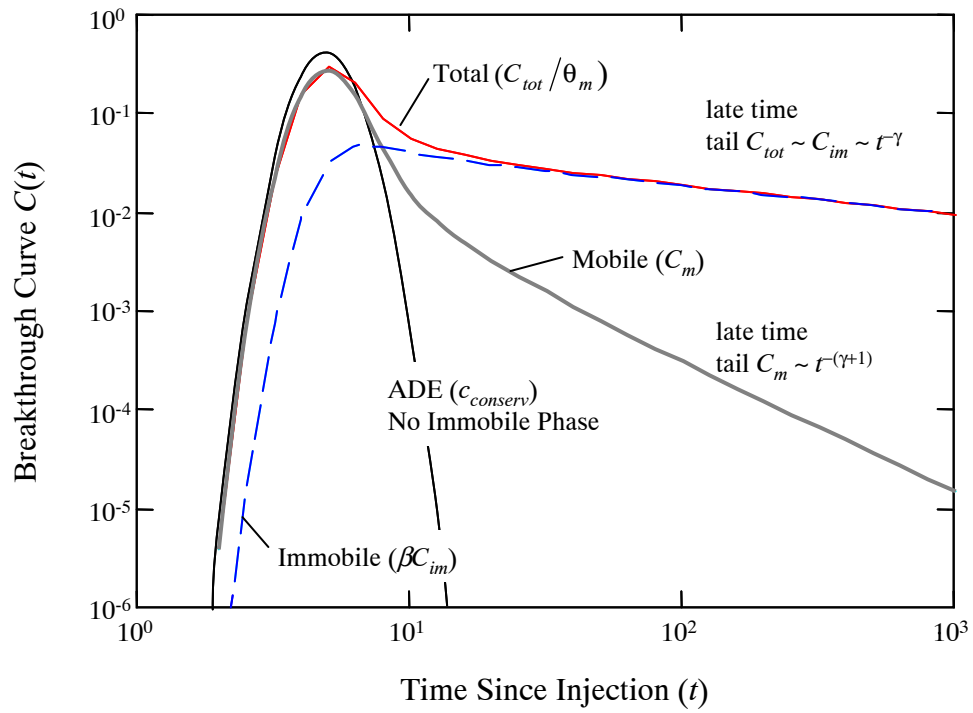


Figure 5. Log-log breakthrough curves, at $x = 5$, of the unretarded solution to the ADE, and the solutions to the total, mobile, and immobile time-fractional ADEs. All parameters are the same as in Figure 1.

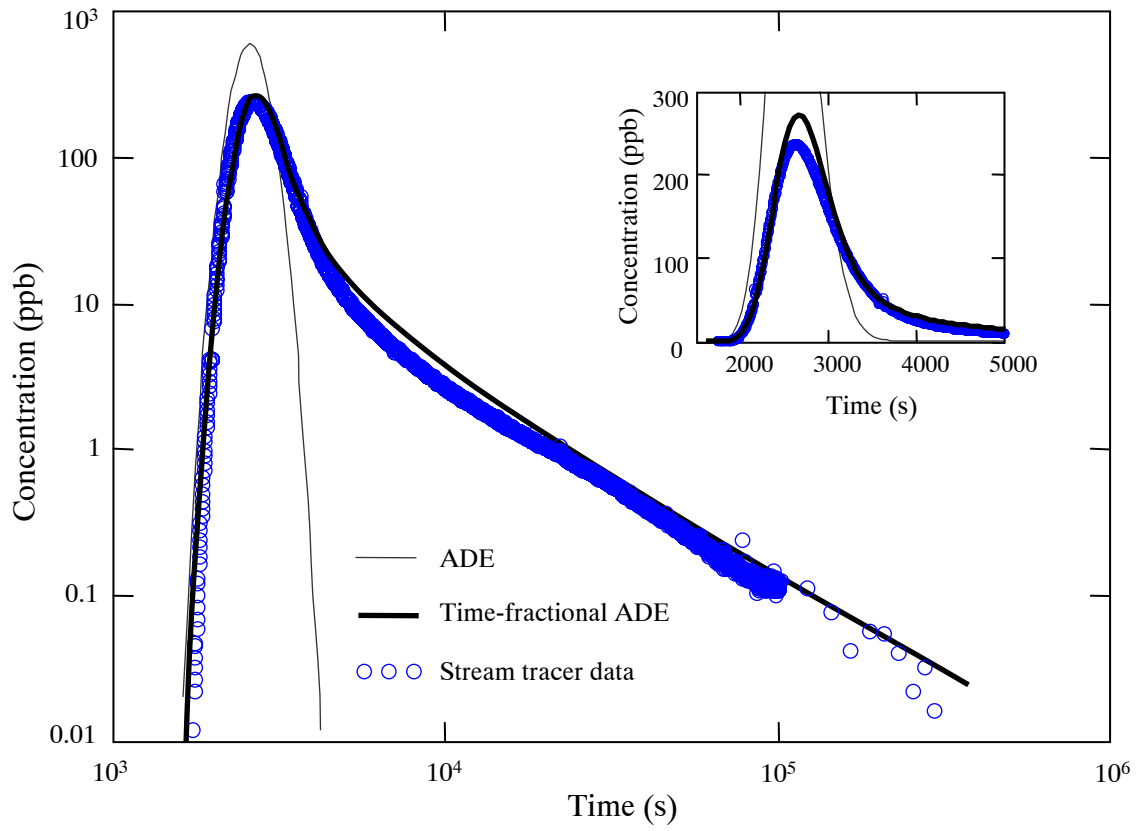


Figure 6. Breakthrough (arrival) of fluorescent dye 306.4 meters downstream of the injection point in a mountain stream.

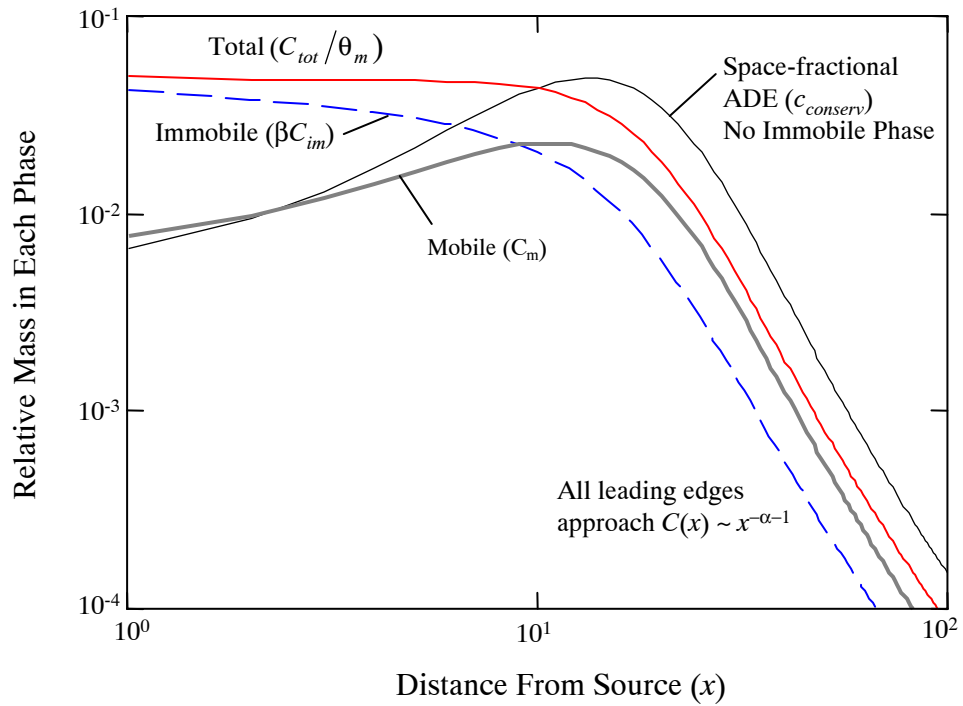


Figure 7. Log-log snapshot, corresponding to Figure 2, at $t = 20$, for the unretarded solution to the fractional-in-space ADE and transformed mobile, immobile, and total solute solutions.

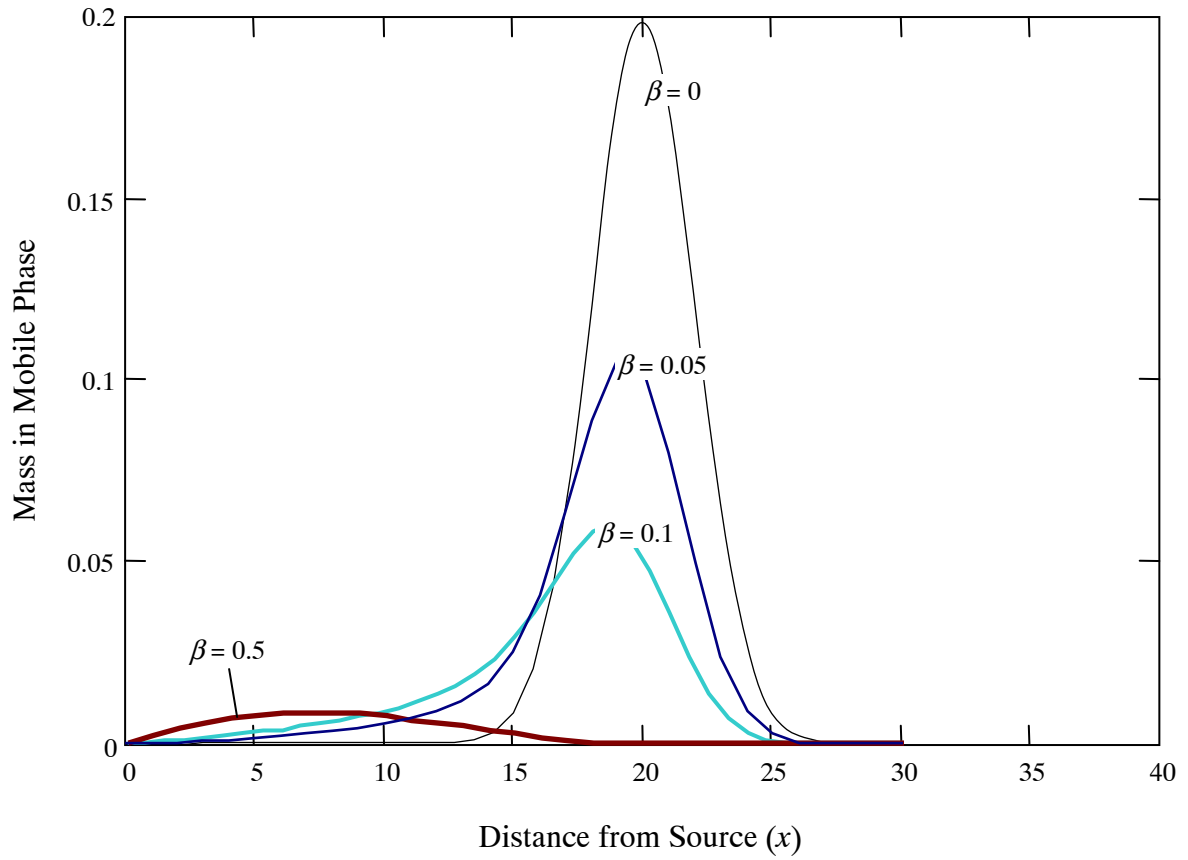


Figure 8. Increasing the capacity coefficient β decreases the mobile mass of the plume and affects the skewness.

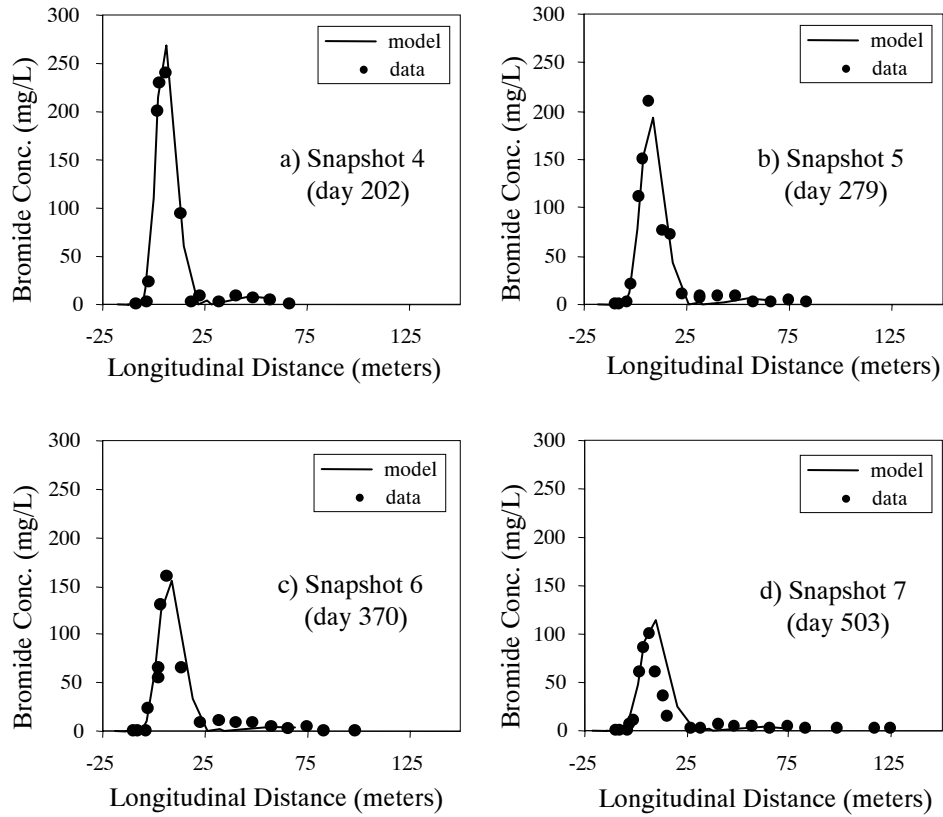


Figure 9. MADE-1 bromide snapshot 3 (day 179) scaled in time by $C_m(x,t) = t^{\gamma-1}t^{-\gamma/\alpha}C_m(t^{-\gamma/\alpha}x,1)$ with $\gamma = 0.33$ and $\alpha = 0.9$ (lines) compared with test data in the final four snapshots (filled circles).